



Published in final edited form as:

*Concepts Magn Reson Part B Magn Reson Eng.* 2010 February 17; 37B(1): 13–19. doi:10.1002/cmr.b.20152.

## New Solenoidal Microcoil NMR Probe Using Zero-Susceptibility Wire

Ravi Kc, Ian D Henry, Gregory H.J. Park, Al Aghdasi, and Daniel Raftery\*

Department of Chemistry, Purdue University, West Lafayette, IN 47907

### Abstract

We present the construction and performance of a 20- $\mu$ L active volume probe that utilizes zero-susceptibility wire for the detection transceiver coil and a 3.5 mm outer diameter thin-wall bubble flow cell to contain the sample. The probe shows good rf homogeneity, resolution, line shape and sensitivity. The sensitivity and resolution of the 20- $\mu$ L probe was compared to those for several other coil configurations, including smaller detection volumes, a thin wire copper coil immersed in susceptibility matching perfluorocarbon FC-43 (fluorinert) fluid, and a standard 5 mm probe. In particular, the  $^1\text{H}$  mass sensitivity,  $S_m$  (SNR per micromole), was 3–4 fold higher than that for the standard 5 mm probe. Finally, the use of the zero-susceptibility wire in smaller volume probes is discussed along with potential future improvements and applications.

### Keywords

Zero susceptibility; solenoid; detection coil; filling factor;  $^1\text{H}$  NMR; microcoil

### Introduction

Nuclear magnetic resonance (NMR) spectroscopy is a premier analytical method for molecular structure determination, is widely used in chemical and pharmaceutical research, and is increasingly used for the analysis of complex samples such as biofluids.<sup>1</sup> However, the sensitivity of NMR can be limiting, which is in part caused by constraints imposed by probe design and sample introduction methods. Thus, sensitivity enhancement methods in NMR are of high interest. Different approaches, such as the use of cryoprobes, sample prepolarisation, optical detection, force detection, induction coupling and the use of microcoil detection have been developed to improve the intrinsic sensitivity of NMR. (2–7)

In microcoil NMR, improved mass-sensitivity,  $S_m$  (SNR per micromole), is achieved by the use of smaller diameter detection coils (7), which capture more magnetic flux lines from the sample and thereby improve the coil efficiency characterized by the ratio of  $B_1/i$ . Further, microcoils that utilize a solenoidal geometry with multiple coil-turns enhance the coil sensitivity compared to a standard NMR probe Helmholtz coil geometry (8). However, as the coil size is reduced and the windings are placed closer to the sample, the magnetic field inhomogeneity in the coil/sample system and its local surrounding increases, which degrades the NMR resolution (9). Thus, both the sensitivity and the resolution issues have to be equally considered in designing high performance NMR probes.

Author to whom correspondence should be addressed: Dr. Daniel Raftery, Professor of Chemistry, Purdue University, Department of Chemistry, 560 Oval Dr., West Lafayette, IN 47907, Office: (765) 494-6070, FAX: (765) 494-0239, raftery@purdue.edu.

Degradation of the spectral resolution by magnetic field inhomogeneity arises mainly due to a susceptibility mismatch in and around the local region of coil including its length, pitch, turns, the sample holder and the sample itself ( $10^{-15}$ ). Since the magnetic flux density is nearly uniform inside a sample with cylindrical or stretched ellipsoidal profiles, any slight mismatch from the sample and the solvent can be perfected using room temperature shimming (14). The rest of the susceptibility mismatch results from the surrounding air, glass and coil material/type. While a variable pitch solenoidal coil is preferred (10), a shorter solenoid with a greater number of turns (11) is best suited for obtaining a homogenous rf magnetic field.

Callahan *et al.* (12) and Fuks *et al.* (13) showed that the magnetic field perturbation of diamagnetic tubes, such as copper and glass, are directly proportional to their volume susceptibility ( $\kappa$ ), thickness and inner radius. Fuks *et al.* elucidated that in order to reduce the tube end-effects on the perturbation field, the lengths of the coil and glass tube should be at least 1–2 folds larger than their diameters for a nearly constant field at the center of the tube. Also, reducing the thickness of the cylinder (i.e. edge-effects from smaller diameter wires and thin glass walls), reduces the amplitude of perturbation proportionally.

Several approaches have been introduced to compensate the susceptibility differences arising from the coil material. Zelaya *et al.* showed that the diamagnetic susceptibility of a copper rod can be reduced by coating paramagnetic rhodium of variable thickness (15). Soffe *et al.* produced zero bulk susceptibility wires made out of rhodium or gold plated copper billet with an aluminum core and constructed a coil for a standard NMR probe at 750-Mhz (16). Unger and Hoult (17) introduced a simple NMR field mapping micro-probe using a long straight wire loop parallel to  $B_0$  that does not create any local  $B_0$  inhomogeneities next to the wire. In their successful microcoil approach, susceptibility matching between the copper coil and the sample was achieved by Olson *et al.* by immersing solenoidal coil/sample system in a perfluorocarbon FC-43 (fluorinert) fluid that has a close susceptibility match to copper (7).

While the use of fluorinert to match the susceptibility of the copper coil has been highly successful in achieving high resolution microcoil probes, its use can lead to somewhat restrictive design considerations. For example, fluorinert based susceptibility matching appears to work best with small diameter copper wire which limits the coil's Q-factor. Fluorinert can limit the the maximum obtainable resonance frequency as it loads the coil significantly. In addition, the temperature range of the probe is limited by the need to keep fluorinert in the liquid phase (8: 18–20).

In this article, we evaluate an alternative approach to match the volume susceptibility of small solenoidal coils. We describe the construction, characterization and performance of a 20- $\mu$ L active volume solenoidal coil bubble-cell NMR flow-probe that features commercially available zero-susceptibility copper wire with an aluminum core used to construct the detection coil. Standard test experiments of the  $^1\text{H}$  rf homogeneity, resolution and lineshape, and  $^1\text{H}$  sensitivity were performed. Using approaches known to provide good static and rf field homogeneity, such as variable pitch coil windings on a thin wall cylindrical pyrex glass sample tube with appropriate coil and sample lengths, excellent probe performance was achieved. High sensitivity was achieved with good resolution and fill factor due in part to the thin glass wall of the sample container. The results of the zero-susceptibility probe at 300 MHz compared very well to a high-sensitive standard 5mm Bruker SEL (single channel direct detection) commercial probe at 300 MHz. A comparison of our probe with a 1.7 mm Bruker probe with a similar active volume (30  $\mu$ L) at 400 MHz is also presented. Solenoidal microcoil flow probes with 1  $\mu$ L active volumes (1.8 mm OD)

were also constructed to test the sensitivity performance of zero-susceptibility wire in smaller volume probes.

The overall aim of this work is to improve both the sensitivity and versatility of microcoil NMR in order to elucidate the mass and volume limited complex samples, such as metabolites in biofluids, tissues, plants or even food extracts. The 20- $\mu\text{L}$  detection-volume allows a good match between the active NMR detection volume and typical chromatographic elution volumes, and the flow probe design allows easy hyphenation of the NMR probe with other analytical systems and modalities, mainly HPLC and mass spectrometry. Finally, the challenges, future improvements and applications of the probes are discussed.

## Methods

### Probe Construction

A 20- $\mu\text{L}$  active volume flow-cell solenoid coil probe was constructed using Cu/Al zero-susceptibility wire (0.53 mm OD; Doty Scientific, Columbia, SC). Construction of the aluminum probe body was similar to our previous work (18·19). To create a 20- $\mu\text{L}$  active volume cell, a section of 5.5 mm OD pyrex glass tube (Chemglass, Vineland, NJ) was stretched, blown and then bent into a U-shape (Fig. 1) to create a 3.5 mm OD bubble sample cell. Bubble-cell etching (18·19) or blowing techniques reduce the total sample amount required by the probe. The sample volume profile inside the Pyrex cell was approximately stretched-ellipsoid with a volume of 58- $\mu\text{L}$  (Fig. 1) and was almost three-fold larger than our previous laser-etched probe referred as the “20- $\mu\text{L}$  larger volume probe (18)”. The typical wall thickness of a blown cell was  $0.3\pm 0.1$  mm measured on a cut cell using a digital caliper (General Tools, NY). For comparison, the wall thickness of the pyrex glass cell in our previous laser-etched probe was measured to be  $2.0\pm 0.2$  mm. A length (65–70 cm) of fused silica capillary transfer line (360  $\mu\text{m}$  OD, 70  $\mu\text{m}$  ID; Polymicro Technologies, Phoenix, AZ) was glued to each end of the sample cell using 5-min epoxy (Devcon, Danvers, MA). The total sample volume required to fill the input and output lines and the bubble cell was approximately 65  $\mu\text{L}$ . The cell volume was measured using a dye filled 100  $\mu\text{L}$  syringe (Hamilton, Reno, NV) (18).

To make a solenoidal coil around the bubble cell, four turns of the zero-susceptibility Cu/Al wire was manually wound around the center portion of the cell using a variable pitch (Fig. 1). Initially, experiments using round zero-susceptibility wire indicated that an inhomogeneity shoulder was apparent for a chloroform shim sample. Therefore, the round wire was flattened to form a rectangular shape using a mallet before winding the coil. The winding pitches of the flattened wire coil were adjusted to cover the active volume and to keep the coil length-to-diameter ratio  $\geq 1:1$ . The two outer turns of the solenoidal coil were glued to the glass cell using a minimal amount of superglue (Henkel Loctite, Rocky Hill, CT).

A single resonant circuit (21·22) that was tuned and matched to a  $^1\text{H}$  frequency of 300 MHz was constructed using the 4-turn sample inductor, two variable capacitors (0.1–9 pF, Voltronics, Denville, NJ), and one fixed-value capacitor (2.2 pF ATC, Huntington Station, NY) as shown in Fig. 1C. The coil inductance was measured to be 109 nH.

### NMR Experiments

1D  $^1\text{H}$  NMR experiments were performed using a Varian INOVA 300 MHz NMR spectrometer and VNMR 6.1C processing software. Standard isotopically enriched solvents, including  $\text{D}_2\text{O}$ , acetone- $\text{d}_6$  and chloroform- $\text{D}$  were purchased from Cambridge Isotope (Andover, MA). Ethyl benzene and chloroform were obtained from Sigma-Aldrich (St.

Louis, MO), and sucrose was purchased from Mallinckrodt Baker (Phillipsburg, NJ). Samples consisting of 1% v/v H<sub>2</sub>O/D<sub>2</sub>O, 1% v/v CHCl<sub>3</sub>/acetone-d<sub>6</sub>, 0.1% v/v ethyl benzene/CDCl<sub>3</sub>, and 100 mM sucrose in D<sub>2</sub>O were prepared for test experiments using standard dilution methods starting at 50% v/v solutions. Prepared samples were injected into the probes using a 100  $\mu$ L Hamilton syringe (Hamilton, Reno, NV) and syringe adapter (VICI Valco, Houston, TX).

After the detection coil was centered in the magnet, the probe was manually shimmed to obtain optimal line width and line shape. The <sup>1</sup>H 90° pulse angle was determined to be 11.6  $\mu$ s at 40dB. For all the small concentration test samples, typical recycle delays of 0.8 s to 1.5 s, and acquisition times from 1.5 to 2.0 sec were chosen to obtain accurate signal to noise ratio (SNR) values. A longer recycle delay time was used for the resolution determination. Standard experiments were performed to evaluate the rf homogeneity, resolution and line shape, and <sup>1</sup>H sensitivity using 1% v/v H<sub>2</sub>O/D<sub>2</sub>O, 1% v/v CHCl<sub>3</sub>/acetone-d<sub>6</sub>, and 0.1% v/v ethyl benzene/CDCl<sub>3</sub> samples, respectively. Also, a single scan 1D <sup>1</sup>H NMR experiment using a 100 mM sucrose in D<sub>2</sub>O sample was performed to compare the sensitivity of the anomeric proton in the thin-wall blown-cell 20- $\mu$ L probe with that of our previous probe that incorporated a laser-etched 20- $\mu$ L volume sample cell (18).

## Results and Discussion

The <sup>1</sup>H resolution for the 20- $\mu$ L active sample volume probe using zero-susceptibility wire was determined at 50%/55%/11% peak height and measured 0.8/30/45 Hz using the 1% v/v CHCl<sub>3</sub>/acetone-d<sub>6</sub> sample (see Fig. 2). In the figure, the baseline resolution and <sup>13</sup>C satellite peaks at natural abundance are shown, along with the whole peak and fit to a Lorentzian line shape in the inset figure. The rf homogeneity results for the probe were determined to be 95% and 88% for the standard 450°/90° and 810°/90° rotation angle ratios, respectively, using the 1% v/v H<sub>2</sub>O/D<sub>2</sub>O sample. Since this sample was undoped, long recycle delay times (~90 sec) were required between 1D <sup>1</sup>H experiments using different flip angles.

The SNR of the probe was determined using a single scan 1D <sup>1</sup>H NMR experiment using 0.1% v/v ethyl-benzene in CDCl<sub>3</sub> (Fig. 3A). The SNR for the quartet methyl peak at 3.4 ppm was 68:1. A noise window of 200 Hz and a line broadening of 0.2 was used in the determination. For comparison, a standard 5 mm 300 MHz Bruker SEL probe was considered. The Bruker SEL probe has SNR=240 (in accordance with the Bruker acceptance specifications) for the approximately 250- $\mu$ L active sample volume. Since conventional probes often have 10–15% higher SNR values than their acceptance specification value, the mass-sensitivity ( $S_m$ , or SNR per micromole) of the solenoidal 20- $\mu$ L probe was therefore determined to be 3–4 fold higher. The molar sensitivity (SNR per unit concentration) of the 20- $\mu$ L probe is comparable to a 1.7 mm 30  $\mu$ L Bruker TXI (<sup>1</sup>H inner coil) flow probe at 400 MHz, which has a <sup>1</sup>H SNR of 75:1 for the same concentration sample. Sensitivity performance of the 20- $\mu$ L probe thin-wall sample-cell probe was also compared with our previous 20- $\mu$ L larger volume probe that had a thicker sample-cell wall<sup>18</sup> and utilized rectangular flat copper wire (~50  $\mu$ m thick) and a susceptibility matching fluid, perfluorocarbon FC-43 (Fluorinert). The SNR for the anomeric proton of sucrose (100 mM sample) at 5.4 ppm using a single scan was measured to be 86:1 (Fig. 3B) for the current 20- $\mu$ L probe. This was 9.4-fold better in sensitivity compared to the previous probe (SNR= 9.2:1).

The sensitivity enhancement observed in our new thin-wall cell using a zero-susceptibility coil over that of our previous probe is mainly due to higher filling factor and the elimination of the long transmission line used in that earlier probe. A sensitivity comparison was made

between the zero susceptibility and thin copper wire coils using the same 3.5 mm OD thin-wall cell in order to keep the fill factor constant. Two parallel copper wires (California Fine Wire, Grover Beach, CA) of 150  $\mu\text{m}$  OD were wound around the cell for three parallel turns, immersed in susceptibility matching fluid (fluorinert), and connected to the tuning/matching capacitors using two 3-cm long semi-rigid 50 $\Omega$  coaxial transmission lines (Haverhill Manufacturing, Haverhill, MA). It was found that the sensitivity of this probe was slightly larger (by 5%) using two parallel wires instead of a single thin wire. Using fluorinert and a piece of semi-rigid coaxial cable increased the coil inductance below the 300 MHz operating frequency. The inter-turn spacings were then adjusted both to obtain the desired frequency, and to cover the 20- $\mu\text{L}$  detection volume. Shown in Table 1, as expected, increasing the turn spacing degraded the resolution. As indicated earlier, the use of a shorter solenoid with multiple turns is preferred to obtain homogenous rf fields. However, fewer turns with large spacings and parallel wire windings were required in order to tune the large coil with 3.5 mm OD to 300 MHz. Improved resolution with copper coils can be obtained by using close-space turns, but the coil length and detection volume (and hence sensitivity) would have to be compromised. For the same 20- $\mu\text{L}$  detection volume the sensitivity of zero-susceptibility coil is slightly better than that for the thin copper wire coil. The degraded sensitivity of the copper coil could be due to in part to the reduced Q-factor of the thin wire, despite the use of two wires in parallel.

We also investigated how the zero-susceptibility wire would perform in smaller volume solenoidal coil geometries. One- $\mu\text{L}$  sample regions were constructed using small fused-silica glass capillaries (1.8 mm OD; Polymicro, Phoenix, AZ) that were etched with 48% hydrofluoric acid (Mallinckrodt AR, Phillipsburg, NJ) using a “quick thermal etching technique” described previously (19). Each etched-sample cell was wound with either zero-susceptibility round wire (3 turns) or 150- $\mu\text{m}$  OD fine copper wire (5 turns) to cover the 1- $\mu\text{L}$  active volume. Photos of these coils are included as Supplemental Information. Each coil was tuned and matched to 300 MHz as described above for the 20- $\mu\text{L}$  active volume sample coil. Line shape and resolution results for the 1- $\mu\text{L}$  solenoidal probes were similar to the 20- $\mu\text{L}$  thin-wall cell probe, although slightly broader line widths of approximately 1.3 Hz at FWHM were observed. As was observed for the larger coil, the sensitivity was slightly better when zero-susceptibility wire was used for the smaller sample volumes.

As is summarized in Table 1, by our construction methods, the zero-susceptibility coil had slightly better sensitivity than the copper coil with fluorinert both for the same thin-wall 3.5mm OD blown cell and the 1.8 mm OD etched cell. However, we stress that the construction efforts employed are not of commercial quality. For the small volume probes, the resolution performance is better using fine wire and fluorinert, which is due to the fact that a better solenoid coil can be wound using a larger number of turns using 150  $\mu\text{m}$  OD copper wire compared to the 0.53 mm OD zero-susceptibility wire on the small capillary. However, at the larger volume the use of zero-susceptibility wire appears to provide better probe performance. We find that very good resolution and sensitivity in a 20- $\mu\text{L}$  active volume probe can be achieved combining zero-susceptibility wire, a stretched ellipsoidal sample profile, and a high fill factor thin wall detection cell.

## Conclusions

The performance of an NMR probe utilizing a zero-susceptibility wire solenoidal coil and a 20- $\mu\text{L}$  active volume was evaluated. The probe provides high resolution that could be obtained by relatively rapid manual shimming. Sensitivity, resolution, line shape, and rf homogeneity for the probe are quite good, especially given the prototype stage of this effort. The mass sensitivity of the probe is higher than larger volume commercial probes but lower than the smaller volume microcoil probes, as could be expected. Compared to the

standard  $^1\text{H}$  non-spin 50/0.55/0.11% peak height resolution specifications of 0.6/6/12 Hz typically for many conventional 5 mm commercial probes, our current probe's resolution is somewhat poorer. However, we anticipate that the probe's resolution can be improved further by optimizing the thickness of the glass and sample shape profile. While the zero-susceptibility coil showed slightly better sensitivity than the thin copper coil in our hands, this difference is not huge. We believe that with optimization of the copper wire diameter and turn spacing, both types of coils can perform equally well. More experimental verification is needed upon the availability of smaller diameter zero susceptibility wire.

One precaution to be noted is that the copper wire is susceptible to oxidation, which could cause a change in the susceptibility matching. This situation was not encountered during this project. However, a slight change in wire-susceptibility due to oxidation may be compensated by adjusting the shim values. Alternatively, a thin layer of paramagnetic material can be coated (12-14) on the copper surface of the zero-susceptibility wire. This will not only prevent oxidation of the wire, but also help adjust the residual susceptibility mismatch of zero-susceptibility wire.

There are a number of future improvements that can be envisioned, such as the optimization of the total sample volume of the probe in the regions outside the active volume, which, in addition to the larger active region, will provide a good approach for structural elucidation on mass limited samples. Ultimately, the ability to use zero-susceptibility wire without any susceptibility-matching fluid may provide an approach towards further sensitivity enhancement by cooling the probe to cryogenic temperatures. Our on-going work is focused on the practical way of minimizing system dead volumes. In addition the probe provides an enhanced match with chromatographic peak elution volumes and the online detection of interesting components in complex samples such as biofluids, plant or nutritional samples. Future studies are focused on detecting individual HPLC separated components from these complex samples for structure elucidation.

## Supplementary Material

Refer to Web version on PubMed Central for supplementary material.

## Acknowledgments

Financial support from the NIH (Grants 1R01GM085291-01 and 1P01AT004511-01) for this project is gratefully acknowledged. We thank Randy Replogle and Pat Mullen of the Precision Machining Facility; and John Pirolo and Bob Gormon of the Chemistry Department Glass Lab for their assistance in this work, as well as the members of the Jon Amy Facility for Chemical Instrumentation.

## References

1. Gowda GAN, Zhang SC, Gu HW, Asiago V, Shanaiah N, Raftery D. Metabolomics-based methods for early disease diagnostics. *Expert Review of Molecular Diagnostics*. 2008; 8(5):617–633. [PubMed: 18785810]
2. Styles P, Soffe NF, Scott CA, Cragg DA, Row F, White DJ, White PCJ. A high-resolution NMR probe in which the coil and preamplifier are cooled with liquid helium. *Journal of Magnetic Resonance*. 1984; 60(3):397–404.
3. Ardenkjaer-Larsen JH, Fridlund B, Gram A, Hansson G, Hansson L, Lerche MH, Servin R, Thaning M, Golman K. Increase in signal-to-noise ratio of > 10,000 times in liquid-state NMR. *Proceedings of the National Academy of Sciences of the United States of America*. 2003; 100(18):10158–10163. [PubMed: 12930897]
4. Savukov IM, Lee SK, Romalis MV. Optical detection of liquid-state NMR. *Nature*. 2006; 442(7106):1021–1024. [PubMed: 16943834]

5. Rugar D, Zuger O, Hoen S, Yannoni CS, Vieth HM, Kendrick RD. Force detection of Nuclear-Magnetic-Resonance. *Science*. 1994; 264(5165):1560–1563. [PubMed: 17769597]
6. Sakellariou D, Le Goff G, Jacquinet JF. High-resolution, high-sensitivity NMR of nanolitre anisotropic samples by coil spinning. *Nature*. 2007; 447(7145):694–697. [PubMed: 17554303]
7. Olson DL, Peck TL, Webb AG, Magin RL, Sweedler JV. High-resolution microcoil H-1-NMR for mass-limited, nanoliter-volume samples. *Science*. 1995; 270(5244):1967–1970.
8. Olson DL, Norcross JA, O'Neil-Johnson M, Molitor PF, Detlefsen DJ, Wilson AG, Peck TL. Microflow NMR: Concepts and capabilities. *Analytical Chemistry*. 2004; 76(10):2966–2974. [PubMed: 15144211]
9. Webb AG, Grant SC. Signal-to-noise and magnetic susceptibility trade-offs in solenoidal microcoils for NMR. *Journal of Magnetic Resonance Series B*. 1996; 113(1):83–87. [PubMed: 8888593]
10. Idziak S, Haerberlen U. Design and construction of a high homogeneity rf coil for solid-state multiple-pulse NMR. *Journal of Magnetic Resonance*. 1982; 50(2):281–288.
11. Peck TL, Magin RL, Lauterbur PC. Design and analysis of microcoils for NMR microscopy. *Journal of Magnetic Resonance Series B*. 1995; 108(2):114–124. [PubMed: 7648010]
12. Callaghan PT. Susceptibility-limited resolution in Nuclear-Magnetic-Resonance microscopy. *Journal of Magnetic Resonance*. 1990; 87(2):304–318.
13. Fuks LF, Huang FSC, Carter CM, Edelstein WA, Roemer PB. Susceptibility, lineshape, and shimming in high-resolution NMR. *Journal of Magnetic Resonance*. 1992; 100(2):229–242.
14. Levitt MH. Demagnetization field effects in two-dimensional solution NMR. *Concepts in Magnetic Resonance*. 1996; 8(2):77–103.
15. Zelaya FO, Crozier S, Dodd S, McKenna R, Doddrell DM. Measurement and compensation of field inhomogeneities caused by differences in magnetic-susceptibility. *Journal of Magnetic Resonance Series A*. 1995; 115(1):131–136.
16. Soffe N, Boyd J, Leonard M. The construction of a high-resolution 750 MHz probehead. *Journal of Magnetic Resonance Series A*. 1995; 116(1):117–121.
17. Unger, PP. Ph.D. Thesis. Winnipeg, Manitoba, Canada: University of Manitoba; 2001. NMR-based Microprobes for magnetic field measurements.
18. Henry ID, Park GHJ, Kc R, Tobias B, Raftery D. Design and construction of a microcoil NMR probe for the routine analysis of 20- $\mu$ L samples. *Concepts in Magnetic Resonance Part B-Magnetic Resonance Engineering*. 2008; 33B(1):1–8.
19. Kc R, Henry ID, Park GHJ, Raftery D. Design and construction of a versatile dual volume heteronuclear double resonance microcoil NMR probe. *Journal of Magnetic Resonance*. 2009; 197(2):186–192. [PubMed: 19138541]
20. Webb AG. Microcoil nuclear magnetic resonance spectroscopy. *Journal of Pharmaceutical and Biomedical Analysis*. 2005; 38(5):892–903. [PubMed: 16087050]
21. Gadian DG, Robinson FNH. Radiofrequency losses in NMR experiments on electrically conducting samples. *Journal of Magnetic Resonance (1969)*. 1979; 34(2):449–455.
22. Murphy-Boesch J, Koretsky AP. An in Vivo NMR probe circuit for improved sensitivity. *Journal of Magnetic Resonance (1969)*. 1983; 54(3):526–532.

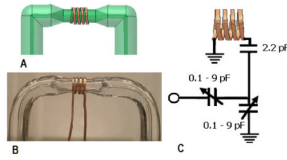


**Figure 1.** (A) Autodesk image of a 20- $\mu\text{L}$  active volume solenoidal coil constructed using 0.53 mm wire; (B) actual image of a typical cell (the stretched-ellipsoidal profile of the sample is somewhat visible); (C) diagram of the single resonant circuit used in the probe.



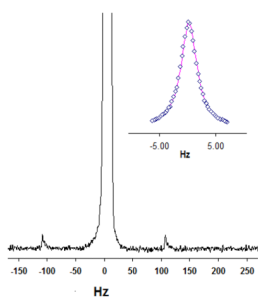


**Figure 2.**

Single scan  $^1\text{H}$  spectrum of 1% v/v  $\text{CHCl}_3/\text{acetone-d}_6$  in the 20- $\mu\text{L}$  active volume thin-wall-cell (3.5 mm OD) zero-susceptibility wire solenoidal coil probe showing the main peak with the  $^{13}\text{C}$  satellite peaks.  $^1\text{H}$  resolution at 50%/.55%/.11% peak height was approximately 0.8/30/45 Hz. The line shape and fit to a Lorentzian function can be seen in the inset figure in which the diamonds represent the experimental data points.

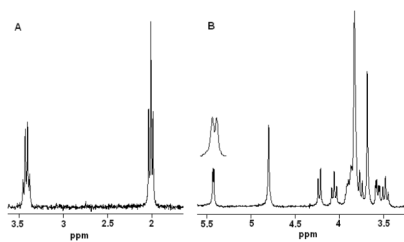


**Figure 3.** (A) Single scan <sup>1</sup>H spectrum of 0.1% v/v ethyl benzene in CDCl<sub>3</sub> for the aliphatic region carried out in the 20- $\mu$ L active volume probe. The SNRs of the quartet (3.4 ppm) and triplet (2 ppm) were 68:1 and 150:1, respectively. (B) Single scan <sup>1</sup>H spectrum of 100 mM sucrose carried out in 20- $\mu$ L probe. The SNR of the anomeric proton was 86:1.

Table 1

Sensitivity and resolution of bubble cell probes constructed with zero-susceptibility wire and fine copper wire immersed in fluorinert.

Sample coil description	Etched Cell OD	Sample profile	<sup>1</sup> H sensitivity (SNR)	<sup>1</sup> H resolution (1% CHCl <sub>3</sub> /CO(CD <sub>3</sub> ) <sub>2</sub> ) (50%/1.55%/-11%)	Mass Sensitivity (S <sub>m</sub> ) EB <sub>1</sub>
20- $\mu$ L zero-susceptibility rectangular wire solenoidal coil.	3.5 mm	stretched ellipsoidal	86:1 (100 mM sucrose); 68:3 (EB <sup>1</sup> )	0.8/30/45 Hz	417
20- $\mu$ L copper coil (fluorinert)	3.5 mm	stretched ellipsoidal	60:1 (EB <sup>1</sup> )	3/70/135 Hz <sup>2</sup>	368
1- $\mu$ L zero- susceptibility round wire solenoidal coil	1.8 mm	ellipsoidal	3:1 (EB <sup>1</sup> )	1.3/78/90 Hz	370
1- $\mu$ L copper coil (fluorinert)	1.8 mm	ellipsoidal	2.8:1 (EB <sup>1</sup> )	0.8/60/80 Hz	340

<sup>1</sup>EB: 0.1% ethyl-benzene quartet;

<sup>2</sup> resolution was compromised by the need to increase the coil's inter-turn spacing for tuning purposes.